Geochemistry Geophysics Geosystems G3
AN ELECTRONIC JOURNAL OF THE EARTH SCIENCES
Published by AGU and the Geochemical Society

Article
Volume 5, Number 8
11 August 2004
Q08L03, doi:10.1029/2004GC000704
ISSN: 1525-2027

Radiometric ages for basement rocks from the Emperor Seamounts, ODP Leg 197

Robert A. Duncan and Randall A. Keller

College of Oceanic and Atmospheric Sciences, Oregon State University, Ocean Administration Building 104, Corvallis, Oregon 97331, USA (rduncan@coas.oregonstate.edu; rkeller@coas.oregonstate.edu)

[1] The Hawaiian-Emperor seamount chain is the "type" example of an age-progressive, hot spot-generated intraplate volcanic lineament. However, our current knowledge of the age distribution within this province is based largely on radiometric ages determined several decades ago. Improvements in instrumentation, sample preparation methods, and new material obtained by recent drilling warrant a reexamination of the age relations among the older Hawaiian volcanoes. We report new age determinations (^{40}Ar-^{39}Ar incremental heating method) on whole rocks and feldspar separates from Detroit (Sites 1203 and 1204), Nintoku (Site 1205), and Koko (Site 1206) Seamounts (Ocean Drilling Program (ODP) Leg 197) and Meiji Seamount (Deep Sea Drilling Project (DSDP) Leg 19, Site 192). Plateaus in incremental heating age spectra for Site 1203 lava flows give a mean age of 75.8 ± 0.6 (2σ) Ma, which is consistent with the normal magnetic polarity directions observed and biostratigraphic age assignments. Site 1204 lavas produced discordant spectra, indicating Ar loss by reheating and K mobilization. Six plateau ages from lava flows at Site 1205 give a mean age of 55.6 ± 0.2 Ma, corresponding to Chron 24r. Drilling at Site 1206 intersected a N-R-N magnetic polarity sequence of lava flows, from which six plateau ages give a mean age of 49.1 ± 0.2 Ma, corresponding to the Chron 21n-22r-22n sequence. Plateau ages from two feldspar separates and one lava from DSDP Site 192 range from 34 to 41 Ma, significantly younger than the Cretaceous age of overlying sediments, which we relate to postcrystallization K mobilization. Combined with new dating results from Suiko Seamount (DSDP Site 433) and volcanoes near the prominent bend in the lineament [*Sharp and Clague*, 2002], the overall trend is increasing volcano age from south to north along the Emperor Seamounts, consistent with the hot spot model. However, there appear to be important departures from the earlier modeled simple linear age progression, which we relate to changes in Pacific plate motion and the rate of southward motion of the Hawaiian hot spot.

Components: 6019 words, 4 figures, 1 table.

Keywords: Hawaiian-Emperor hot spot track; ^{40}Ar-^{39}Ar geochronology; hot spot motion.

Index Terms: 8121 Tectonophysics: Dynamics, convection currents and mantle plumes; 8155 Tectonophysics: Plate motions—general; 9355 Information Related to Geographic Region: Pacific Ocean.

Received 27 January 2004; **Revised** 22 April 2004; **Accepted** 16 May 2004; **Published** 11 August 2004.

Duncan, R. A., and R. A. Keller (2004), Radiometric ages for basement rocks from the Emperor Seamounts, ODP Leg 197, *Geochem. Geophys. Geosyst.*, *5*, Q08L03, doi:10.1029/2004GC000704.

Theme: Movement, Dynamics, and Geochemical Evolution of the Hawaiian Hot Spot
Guest Editors: R. Duncan, J. A. Tarduno, D. Scholl, and T. Davies

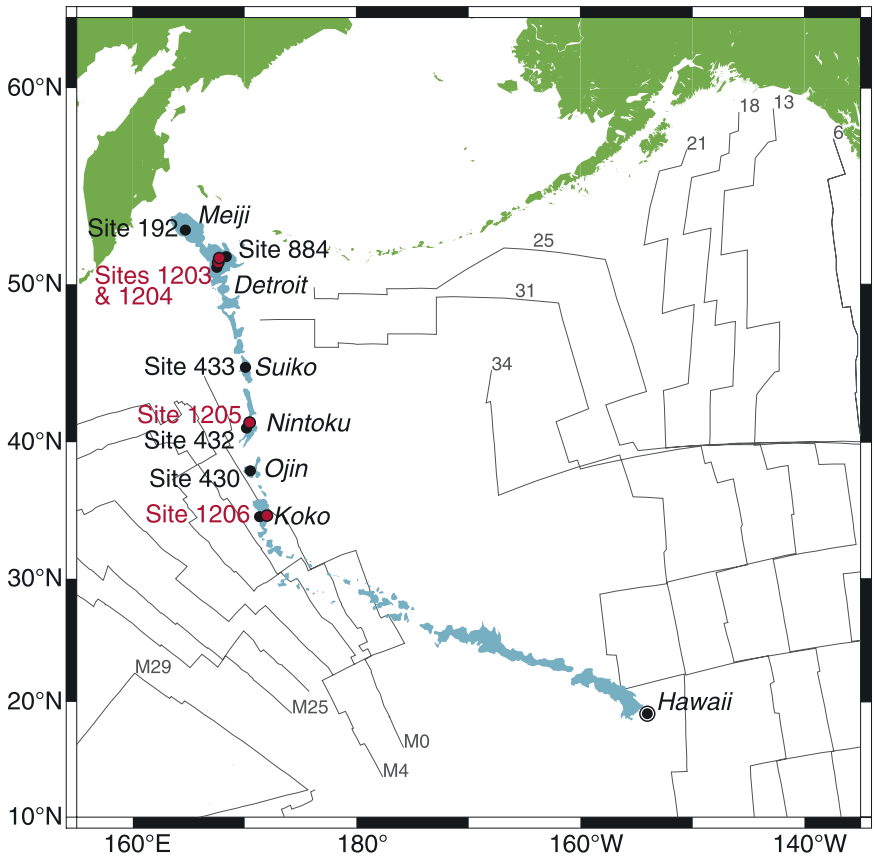

Figure 1. Location of ODP Leg 197 drill sites (in red), all in the Emperor seamount chain, northwestern Pacific Ocean. Shown also are previous DSDP and ODP drilling sites (in black) on this volcanic lineament. Precise radiometric ages and paleolatitudes from these sites form the basis of the test of Hawaiian hot spot movement during the formation of the Emperor Seamounts.

1. Introduction

[2] A key element in fulfilling several ODP Leg 197 science objectives is determining the age of volcanic activity at different locations along the Emperor seamount chain (Figure 1). We have determined crystallization ages using ^{40}Ar-^{39}Ar incremental heating experiments, for whole rocks and feldspars separated from basement units recovered at Sites 1203, 1205, and 1206 and alteration ages from Site 1204 and DSDP Site 192. The main objective of Leg 197 drilling is to determine the paleolatitude history of the Hawaiian hot spot. To do this requires accurate and precise ages for the acquisition of the natural remnant magnetization measured for lava flows from the three volcanic systems sampled. The radiometric method of choice for these lava flow compositions, in this age range, with the observed low temperature alteration is ^{40}Ar-^{39}Ar incremental heating. Basement ages also contribute to calibration of biostratigraphic data, assessment of the timescale of physical volcanic processes, magma production rates and hot spot/plume dynamics in the period of construction of the Emperor Seamounts.

[3] Previous radiometric dating of the Emperor Seamounts has been limited to K-Ar and ^{40}Ar-^{39}Ar ages of dredged samples from several volcanoes [*Clague and Dalrymple*, 1973, 1987] and cored samples from Nintoku, Ojin and Suiko Seamounts [*Dalrymple et al.*, 1980a], Detroit Seamount [*Keller et al.*, 1995] and Meiji Seamount [*Dalrymple et al.*, 1980b]. These data are summarized in Figure 3. However, Leg 197 is notable in the deep penetration achieved at each volcano, with the recovery of material from potentially significantly longer periods of volcano construction than that sampled by dredges from the surface or shallow penetration drilling sites. Evidence from several sites, in the form of stratigraphic breaks, such as physical evidence of submergent to emergent conditions of

lava flow emplacement, soil zones, and magnetic reversals, suggests that geologically significant periods of time may be represented in the cored material. Hence, we believed it important to apply radiometric dating to as many distinct cooling units (identified geochemically, magnetically and by observations of physical volcanology) as practical.

[4] Another consideration is the potential for nonlinear hot spot movement expressed in the age-distance relationship (Figure 3). Previous age determinations from the Emperor Seamounts appear to fit an approximately linear age progression with little, if any, discernable change in plate velocity at the Hawaiian-Emperor bend [*Dalrymple et al.*, 1980a]. However, this may be fortuitous given the mix of volcanic stages sampled (tholeiitic and alkali basalt compositions among the dated dredged and cored samples) and the small number of age determinations (1 or 2 per volcanic system). Work in progress by *Sharp and Clague* [2002] indicates both a wider age range in volcanic activity at some seamounts near the Hawaiian-Emperor bend and inaccuracies in previously reported ages, which require changes in Pacific plate over hot spot velocities. From the conclusion, based on paleomagnetic analyses of Leg 197 cores, that southward motion of the Hawaiian hot spot may have been faster in the early history of Emperor Seamount formation, slower toward the Hawaiian-Emperor bend, and almost negligible during the Hawaiian Ridge formation [*Tarduno et al.*, 2003], we anticipate that apparent Pacific plate velocities may vary with time. It should be possible to examine this dynamic aspect of hot spot/plume behavior through radiometric dating of a common stage of volcano development (the waning phases of the tholeiitic shield stage), now sampled at Detroit, Suiko, Nintoku, Ojin and Koko Seamounts.

2. Analytical Work

2.1. Sample Selection and Coverage

[5] We made an initial assessment of sample suitability for dating onboard the drilling ship by thin section examination of from 1 to 2 slides per unit. Good quality material, as judged by well crystallized texture, extent of alteration, low total alkalis and loss on ignition (shipboard measurements), is available at Sites 1205 and 1206, while more altered rocks occur at Sites 1203 and 1204. Because of significant compositional changes and evidence for time breaks down-core at most sites, we sampled every unit that contained datable material.

2.2. Sample Preparation

[6] A time-consuming, but critical aspect of precise and unambiguous age results is isolation of optimum material for radiometric dating. We prepared samples in a variety of ways, depending on mineralogy, texture and evidence of alteration. Aphyric rocks with small but pervasive amounts of groundmass alteration (clay) were prepared by drilling minicores (4 mm diameter) from the freshest interiors of sawn surfaces. These minicores were then sliced into ~100 mg disks using a diamond-impregnated fine bandsaw, and marked for identification. Vesicular rocks, which commonly contained clay, zeolite and carbonate fillings, were avoided. Feldspar-porphyritic rocks were crushed, sieved and separated using a Frantz isodynamic magnetic separator. We then treated the feldspar concentrates with a mild acid leaching procedure to remove small amounts of clay and adhering groundmass. This consisted of a wash in 5% HF for 30 seconds, water rinse, ultrasound in dilute nitric acid for 20 min, water rinse, then drying. We examined the cleaned separates with a binocular microscope and removed remaining altered crystals by hand. Cleaned feldspar separates were wrapped in Cu-foil and marked for identification.

[7] Samples, both whole rock disks and Cu-wrapped feldspar separates, were stacked in quartz vials and loaded in an irradiation tube. We monitored the neutron fluence of the Oregon State University TRIGA research reactor with the Fish Canyon Tuff biotite standard (28.03 ± 0.16 Ma [*Renne et al.*, 1998]), spaced at regular intervals among the sample unknowns. Errors in monitor measurements and gradient fitting accumulated to about 0.5%. Typical irradiation conditions were 6 hours in a dummy fuel rod in the reactor's central ring, at 1 MW power.

2.3. Methods

[8] Following irradiation and initial decay of short-lived radionuclides, we loaded the samples in two ultra-high vacuum gas extraction lines. The first is a double-vacuum resistance furnace with thermocouple-controlled Ta-crucible (internal Mo-sleeve). Whole rock disks were analyzed one after another from a drop-in manifold. The second is a laser microprobe that employs a computer-controlled moving stage beneath a 10W CO_2 laser to heat

multiple grains in an incremental heating mode. We analyzed the feldspar separates with the laser system. After gas clean-up with Zr-Al getters we measured the isotopic composition of Ar released at each heating step with a MAP 215/50 mass spectrometer. Samples were heated in 50–100°C increments, from 400°C to fusion in 6 to 13 steps, depending on K-content.

[9] The Ar data were acquired in a peak-hopping mode (for m/z = 35, 36, 37, 38, 39, 40) by computer. Peak decay was linear and typically <10% over 12 sets of peaks and backgrounds. Mass discrimination on the MAP system was measured with zero age samples run in the same way as samples, and was constant at 1.005 (for 2 a.m.u.). The sensitivity of the mass spectrometer is 4×10^{-14} mol/V and measured backgrounds were 1.5×10^{-18} mol at m/z = 36, 2×10^{-18} mol at m/z = 39 and 1.5×10^{-16} mol at m/z = 40. Procedure blanks for the resistance furnace ranged from 3.0×10^{-18} mol ^{36}Ar and 9.0×10^{-16} mol ^{40}Ar at 600°C to 6.4×10^{-18} mol ^{36}Ar and 1.9×10^{-15} mol ^{40}Ar at 1400°C, while laser chamber blanks measured before each sample and after every third step during sample analysis were 2 to 3×10^{-18} mol ^{36}Ar and 6 to 9×10^{-16} mol ^{40}Ar [*Duncan*, 2001].

3. Results

[10] Mass spectrometric data are summarized in Table 1, and presented graphically in Figures 2a–2j. Complete experimental data and plots are available in electronic files, which may be downloaded from the EarthRef Digital Archive (ERDA) at http://earthref.org/ and following the Quick Links, or on request from the first author. We used the ArArCALC v2.2 software from *Koppers* [2002] to reduce data and make plots. Isotopic ratios, determined from regression of the Ar mass peak heights with time, are used in two ways. Step ages were calculated, using the corrected *Steiger and Jager* [1977] decay constant of $5.530 \pm 0.097 \times 10^{-10}$ yr^{-1} (2σ) as reported by *Min et al.* [2000], assuming that initial sample Ar compositions were atmospheric (initial ^{40}Ar/^{36}Ar = 295.5), and plotted against cumulative proportion of gas released (percent ^{39}Ar) as age spectrum, or "plateau" diagrams. Alternatively, isotope correlation diagrams (^{40}Ar/^{36}Ar versus ^{39}Ar/^{36}Ar) were examined for colinear step compositions whose slope is equivalent to age since closure to gas diffusion (crystallization) and whose ^{40}Ar/^{36}Ar intercept reveals the initial Ar composition of the rock or mineral at closure. We accept an apparent age as an accurate estimate of the sample crystallization age if several statistically testable conditions are met [*Dalrymple et al.*, 1980a; *Pringle and Duncan*, 1995], namely:

[11] 1. A well-defined, mid- to high-temperature plateau is formed by at least three concordant, consecutive steps representing >50% of the total ^{39}Ar released; the plateau age is the weighted mean of these step ages, using $1/\sigma^2$ as the weighting factor.

[12] 2. A well-defined isochron exists for the same plateau step compositions; the isochron is fit using the YORK2 weighted least squares regression with correlated errors [*York*, 1969].

[13] 3. The plateau and isochron ages are concordant.

[14] 4. The isochron ^{40}Ar/^{36}Ar intercept is atmospheric composition.

[15] The plateau and isochron fits were evaluated by the mean square of weighted deviations (MSWD in Table 1), which is an F statistic whose maximum value for significance is about 2.7.

[16] Whole rock and feldspar separates from three of the four ODP Leg 197 drill sites presented in Table 1 meet the criteria listed above. Plateau ages (2σ uncertainties) are the mean of between three and nine step ages, representing >50% of the total sample ^{39}Ar. Corresponding isochron ages are concordant, although they sometimes have significantly larger uncertainties because of the small dispersion of step isotopic compositions. ^{40}Ar/^{36}Ar intercepts are, with two barely significant exceptions, within analytical uncertainty of the atmospheric value, and the two departures are again due to fitting small numbers of closely grouped points in isotope correlation space. Total fusion ages, obtained by summing all step compositions for a given experiment, are roughly equivalent to a conventional K-Ar age. Results for each site are next evaluated.

3.1. Site 1203 (Detroit Seamount)

[17] The volcanic basement at Site 1203 was reached beneath 462 m of diatom and nannofossil oozes and chalks. Biostratigraphic examinations on board ship determined that sediments intercalated with submarine-erupted lava flows are 75–76 Ma (nannofossil zone cc22 [*Shipboard Scientific Party*, 2002]). Paleomagnetic measurements added the information that these rocks

Table 1. The ^{40}Ar-^{39}Ar Radiometric Ages for the Emperor Seamounts[a]

Sample	Material	Total Fusion Age, Ma	2σ Error	Plateau Age, Ma	2σ Error	N	MSWD	Isochron Age, Ma	2σ Error	$^{40}Ar/^{36}Ar$ Initial	2σ Error	J
					Detroit Seamount							
1203-19R-2, 136-138	feldspar	23.90	0.18	none developed				none developed				0.001583
1203-31R-1, 29-31	feldspar	29.72	1.00	none developed				none developed				0.001526
1203-32R-5, 58-60	whole rock	74.36	0.53	75.55	0.89	3/6	3.52	76.41	2.91	285.1	32.4	0.001691
1203-35R-4, 93-95	feldspar	72.64	2.85	76.27	2.76	4/6	0.36	75.53	3.98	298.3	11.1	0.001495
1203-36R-4, 102-106	feldspar	58.66	2.65	71.19	5.93	3/6	2.19	*66.07*	*6.91*			0.001798
1203-38R-1, 129-131	whole rock	75.52	1.21	75.14	1.16	5/9	1.65	74.63	2.06	296.7	4	0.001676
1203-59R-2, 102-103	whole rock	76.23	1.24	77.73	1.44	6/8	1.70	75.23	2.36	300.2	3.9	0.001704
				75.82[b]	**0.61**[c]							
1204-2R-2, 93-95	whole rock	48.61	0.29	none developed				none developed				0.001638
1204-9R-1, 92-94	feldspar	47.20	1.20	47.60	0.78	4/12	1.90	47.25	1.38	302.5	34.1	0.001414
1204-9R-1, 92-94	whole rock	58.06	0.91	none developed				none developed				0.001664
1204-14R-2, 131-134	feldspar	36.78	0.34	none developed				none developed				0.001439
1204-14R-2, 131-134	whole rock	49.97	0.73	none developed				none developed				0.001621
1204-14R-3, 67-69	whole rock	52.35	1.65	none developed				none developed				0.001651
1204-17R-1, 89-92	feldspar	32.52	0.12	none developed				none developed				0.001786
					Nintoku Seamount							
1205-5R-2, 30-34	whole rock	55.13	0.64	55.12	0.61	5/10	0.61	55.16	0.72	299.4	44.2	0.001544
1205-6R-1, 0-4	whole rock	55.26	0.71	55.33	0.63	3/11	1.02	54.57	1.24	385.2	126.6	0.001517
1205-6R-2, 25-28	feldspar	56.58	0.35	55.21	0.45	5/7	2.63	55.00	0.50	303.0	14.9	0.001576
1205-10R-2, 73-75	whole rock	54.69	0.61	55.28	0.61	8/13	1.82	55.27	0.63	295.4	12.8	0.001582
1205-20R-5, 60-65	whole rock	52.90	0.58	55.20	0.61	7/13	1.12	55.62	1.17	202.4	182.9	0.001567
1205-39R-1, 70-72	whole rock	56.33	0.57	56.37	0.57	9/10	1.80	56.25	0.57	299.6	3.4	0.001557
1205-45R-1, 123-126	whole rock	56.26	0.62	56.22	0.63	6/12	2.15	56.27	0.64	283.0	21.7	0.001531
				55.51[b]	**0.22**[c]							
					Koko Seamount							
1206-3R-2, 116-118	whole rock	46.93	1.20	48.53	0.73	4/8	0.25	48.72	1.00	294.7	2.8	0.001747
1206-10R-1, 0-3	whole rock	46.51	2.32	48.70	1.16	7/8	1.01	49.52	1.47	293.3	2.5	0.001754
1206-15R-4, 37-40	whole rock	51.17	0.45	49.45	0.50	4/9	1.61	50.57	1.05	203.9	78.8	0.001712
1206-20R-3, 70-72	whole rock	48.59	0.47	48.34	0.41	5/9	0.54	48.35	0.64	292.6	21.5	0.001765
1206-24R-3, 37-39	whole rock	50.15	0.59	49.53	0.47	6/8	0.79	49.88	0.77	288.7	11.4	0.001738
1206-41R-1, 9-12	whole rock	30.50	0.27	none developed				none developed				0.001721
1206-44R-2, 120-125	whole rock	48.73	0.41	49.69	0.39	4/8	0.24	49.97	0.72	257.1	83.8	0.001729
				49.16[b]	**0.21**[c]							

Table 1. (continued)

Sample	Material	Total Fusion Age, Ma	2σ Error	Plateau Age, Ma	2σ Error	N	MSWD	Isochron Age, Ma	2σ Error	$^{40}Ar/^{36}Ar$ Initial	2σ Error	J
				Meiji Seamount								
192-6R-2, 7-14	feldspar	37.67	0.16	37.90	0.16	7/13	1.71	37.93	0.31	289.6	46.2	0.001798
192-6R-2, 75-81	whole rock	41.24	0.25	33.21	0.18	4/8	2.22	33.09	0.64	301.8	31.5	0.001773
192-6R-3, 3-9	feldspar	33.71	0.16	33.80	0.15	6/10	1.32	33.64	0.25	320.1	31.6	0.001639

[a] Ages calculated using biotite monitor FCT-3 (28.04 Ma) and the total decay constant λ = 5.530E-10/yr. N is the number of heating steps (defining plateau/total); MSWD is an F statistic that compares the variance within step ages with the variance about the plateau age. J combines the neutron fluence with the monitor age.
[b] Mean plateau age.
[c] Mean 2σ error.

acquired a remanent magnetization during a period of normal polarity, which is consistent with the fossil age estimate. Seven samples were selected from the 453 m cored basement section for age determinations, five of which produced acceptable crystallization ages. The two uppermost samples are plagioclase-olivine-phyric basalts that contain zoned and partially altered (to clay) feldspars in a fine-grained matrix altered to clay and carbonate. These produced discordant age spectra and total fusion ages of 20–22 Ma. Deeper in the cored section the lavas become more aphyric and are considerably less altered. These rocks provided consistent ages with a mean of 75.82 ± 0.62 Ma, which agrees well with the fossil evidence.

[18] Figures 2a and 2b illustrate two examples of acceptable plateaus and concordant isochrons. Compositionally, these lavas are tholeiitic to transitional at the top of the section, while alkali basalts are intercalated with tholeiitic basalts downsection. Low K contents in some units and relatively pervasive alteration led to poor precision (low proportions of radiogenic Ar) in some analyses. We cannot detect any significant difference in age through this cored section. Our measured ages are significantly younger than the 81 Ma plateau age reported by *Keller et al.* [1995] from an ODP Site 884 tholeiitic basalt lava flow. The reverse polarity magnetization of flows at that site is consistent with the reported age and an older magnetic chron than observed at Site 1203. That site is ~48 km to the northeast of Site 1203, and located much deeper (3826 m) on the flank of the Detroit volcanic platform, so a strong possibility exists that Site 884 is located on an older volcano which we refer to as Detroit north.

3.2. Site 1204 (Detroit Seamount)

[19] Similar to evidence at Site 1203 the biostratigraphic data for lowermost sediments indicate a minimum age for Site 1204 of 71–76 Ma (nannofossil zones cc22-cc23 [*Shipboard Scientific Party*, 2002]). However, none of the seven samples analyzed from Site 1204 produced acceptable crystallization ages. Age spectra are discordant; no plateaus developed and consequently no isochrons could be constructed. Figure 2c presents an example of such a discordant spectrum. Four of the 12 steps from feldspar sample 1204-9R-1, 92–94 cm produced a consistent age of about 48 Ma. In view of the low proportion of gas

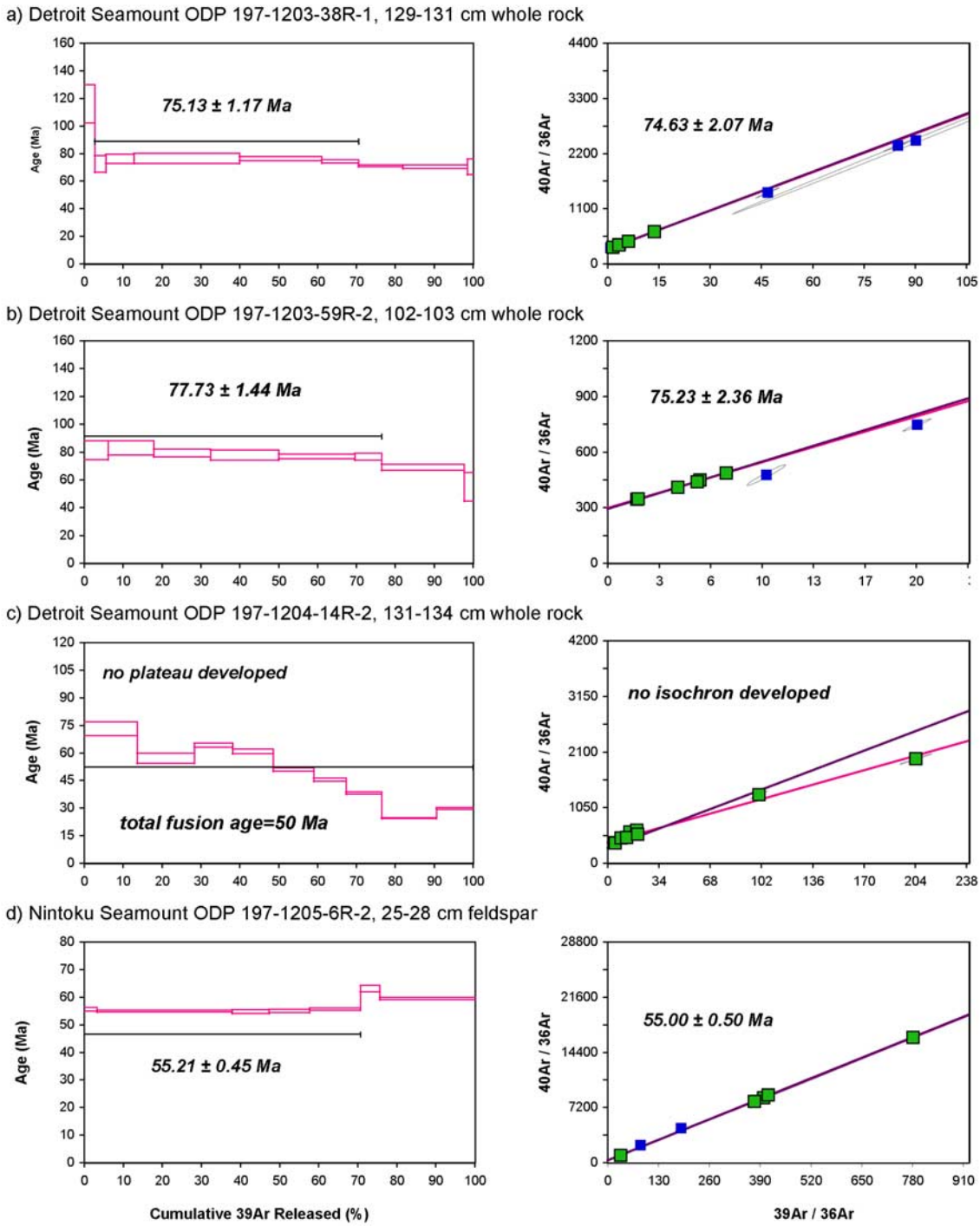

Figure 2. Representative age spectra and isochron plots for ^{40}Ar-^{39}Ar incremental heating experiments on whole rocks and feldspars from the Emperor Seamounts. (a and b) Detroit Seamount (Site 1203), (c) Detroit Seamount (Site 1204), (d, e, and f) Nintoku Seamount (Site 1205), (g and h) Koko Seamount (Site 1206), and (i and j) Meiji Seamount (DSDP Site 192). The green squares in the isochron plots (boxes on the right) indicate those step gas compositions used in the regression (plateau steps), while the blue squares are steps omitted.

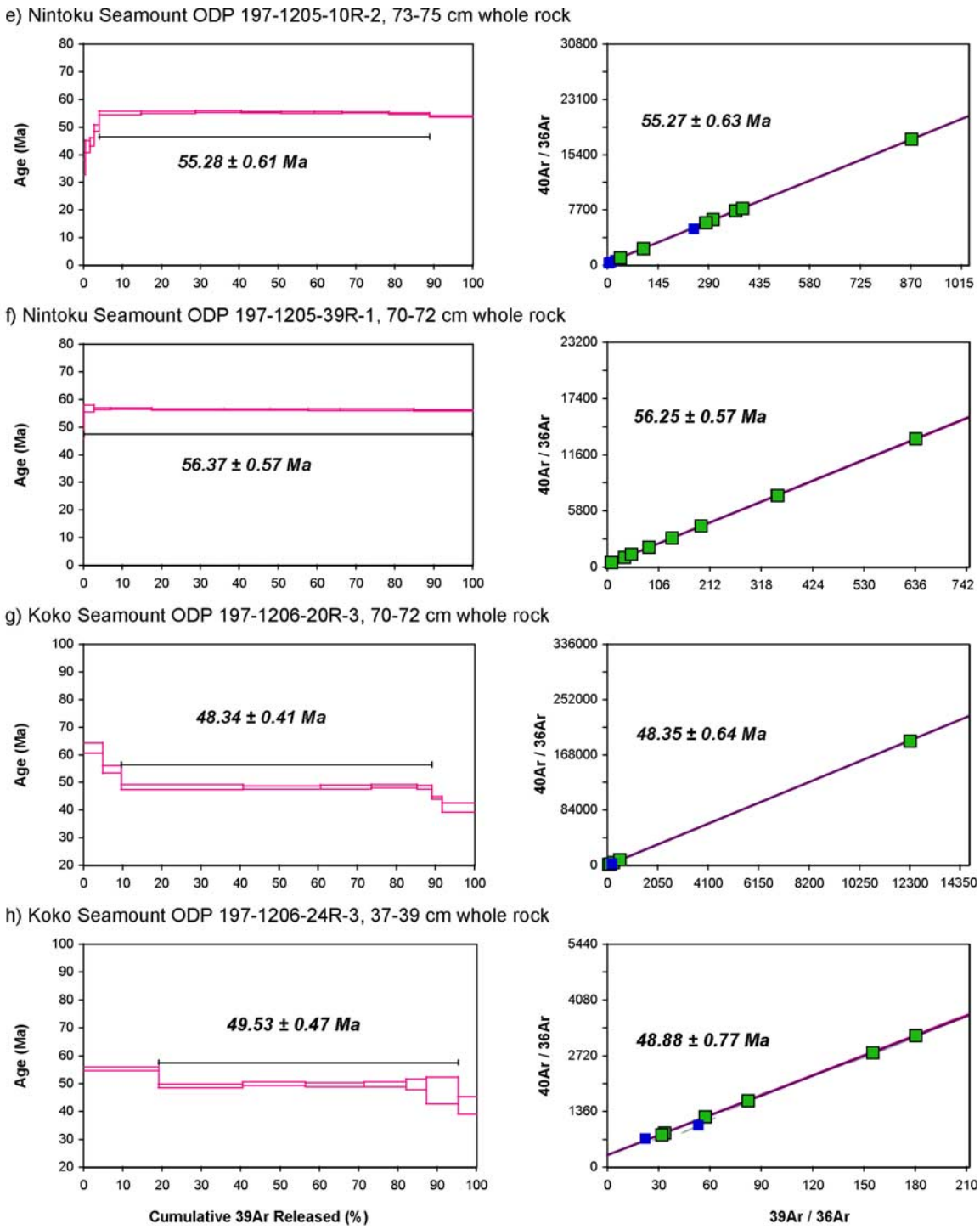

Figure 2. (continued)

released in these steps (43% of total) we do not consider this an acceptable crystallization age. Total fusion ages for the seven samples range from 33 to 58 Ma. Likewise, *Keller et al.* [1995] found only discordant age spectra from ODP Site 883 lavas, located ~0.5 km to the northwest; total fusion ages for two such samples are 50–52 Ma.

[20] The cored volcanic section at this site consists dominantly of aphyric to sparsely plagioclase-phyric lavas, with glassy matrix (now altered to clay and carbonate). We conclude that low temperature alteration of the poorly crystallized matrix and concurrent ^{40}Ar loss, together with K addition, was responsible for the non-

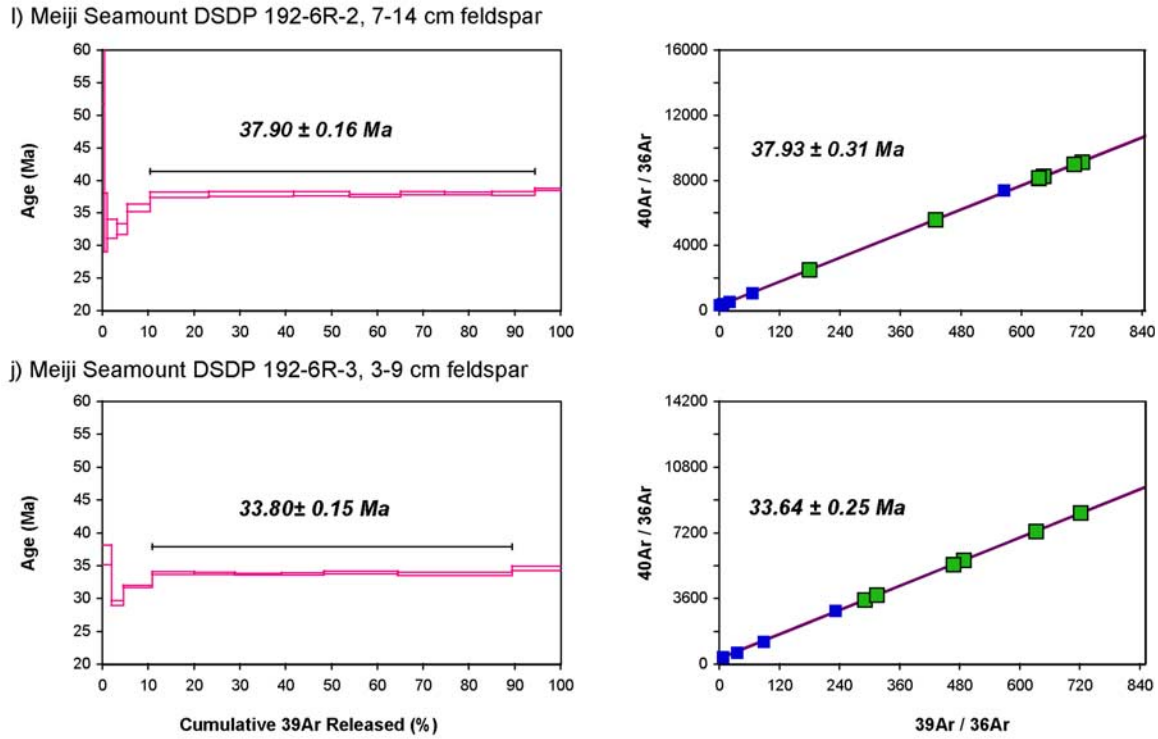

Figure 2. (continued)

ideal age spectra and total fusion ages significantly less than biostratigraphic age estimates. Within the lower 50 m of the thick (814 m) carbonate sediments overlying the basement lava flows are Eocene chalks containing numerous volcanic ashes that have been deformed by rotation and sliding. B. C. Kerr et al. (Seismic stratigraphy of Detroit Seamount, Hawaiian-Emperor seamount chain: Deposition of the Meiji Drift and implication for post–hot spot shield-building volcanism, submitted to *Geochemistry, Geophysics, Geosystems*, 2004) note seismic imaging of volcanic features that postdate the original construction of the seamount, and conclude that local tectonism and volcanism modified portions of Detroit Seamount in the Eocene. These events are likely the cause of the disrupted K-Ar system observed at this site, and the Eocene total fusion ages.

3.3. Site 1205 (Nintoku Seamount)

[21] All volcanic units at Site 1205 are reversely magnetized and the biostratigraphic data for lowermost sediments indicate an early Eocene age, 54–55 Ma (nannofossil zone NP10 [*Shipboard Scientific Party*, 2002]). Drilling here penetrated 283 m of mildly alkalic, subaerially erupted, only slightly altered lava flows beneath a 42 m sedimentary cover that included rounded cobbles of hawaiite composition. Numerous well-developed soil horizons were recovered, indicating that significant periods occurred between eruptions, possibly during the waning stage of shield construction. Plateau ages from six whole rocks (including one of the hawaiite cobbles) and one feldspar separate spanning the cored basement section at this site give a mean age of 55.50 ± 0.22 Ma, corresponding to Chron 24r [*Berggren et al.*, 1995]. Figures 2d, 2e, and 2f give three examples of excellent plateau ages and corresponding isochrons. Although plateau ages rise from 55.2 to 56.2 Ma downsection, there is no statistically significant difference in age between the top and bottom of the section. Our ages are compatible with the isochron age reported by *Dalrymple et al.* [1980a], 56.2 ± 0.6 Ma, for a lava flow from DSDP Site 432, located only ~100 m to the northwest of Site 1205.

3.4. Site 1206 (Koko Seamount)

[22] Drilling at Site 1206 penetrated 57 m of shallow water (reefal) sediments and intersected a 278 m N-R-N magnetic polarity sequence of tholeiitic to mildly alkali basalt lava flows, interpreted to have been erupted in shallow

submarine to subaerial conditions. The biostratigraphic data for lowermost sediments at Site 1206 indicate a middle Eocene age, 44–50 Ma (nannofossil zones NP14 and 15 [*Shipboard Scientific Party*, 2002]). A previously reported ^{40}Ar-^{39}Ar plateau age of 48.1 Ma comes from a dredged rock nearby [*Clague and Dalrymple*, 1973]. Six of seven whole rock samples selected for dating produced acceptable plateau ages, which give a mean age of 49.15 ± 0.21 Ma, corresponding to the Chron 21n-22r-22n sequence. Figures 2g and 2h illustrate two examples of plateaus and isochrons. Age differences between top and bottom of the dated section are barely significant and indicate a total age range of 0.5–1.0 myr, consistent with the paleomagnetic data.

3.5. Site 192 (Meiji Seamount)

[23] The northwesternmost volcanic center in the intact Hawaiian-Emperor chain is Meiji Seamount (Figure 1). Site 192 was drilled during DSDP Leg 19, where 13 m of altered basalt were penetrated beneath 1044 m of diatom ooze, clays, and carbonate sediments, the lowermost of which are Maastrichtian age (68–70 Ma [*Creager et al.*, 1973]). *Dalrymple et al.* [1980b] previously reported a minimum age for Meiji Seamount of 62 Ma, based on conventional K-Ar analyses and ^{40}Ar-^{39}Ar incremental heating data. In an attempt to obtain better information about the crystallization age and alteration history of Meiji Seamount, we resampled the archived core material. The five pillow lava flows recovered from Site 192 are extensively altered: groundmass contains clay, carbonate, zeolite and secondary iron oxide, while plagioclase feldspar has been variably replaced by K-feldspar. *Dalrymple et al.* [1980b] speculate that this replacement is due to low-temperature, K-rich fluids produced during alteration of the basalts. We separated feldspar from two samples and selected a single well-crystallized whole rock for a third experiment. All three produced acceptable plateaus and isochrons between 33 and 38 Ma, indicating complete resetting of the K-Ar system during K-metasomatism. We are no closer to knowing the formation age of Meiji Seamount but we can now constrain the timing of the metamorphic event that drove fluids through the seamount to the late Eocene. Whether this occurred as a result of nearby tectonic and volcanic activity (as suspected at Site 1204) or rapid thickening of overlying sediments cannot be judged.

4. Discussion and Conclusions

[24] The new age results provide important information for the principal objective of ODP Leg 197, namely, the paleomagnetic test of Hawaiian hot spot motion relative to the geomagnetic dipole field [*Tarduno et al.*, 2003]. The latitude of the hot spot, inferred from paleoinclination data, changed from about 34°N at Detroit Seamount to about 21°N at Koko Seamount. Together with the ages of volcanic activity the data imply a southward motion of the hot spot of 4.3 (±2.3) cm/yr between 81 and 49 Ma relative to the geomagnetic dipole field. From 49 Ma to the present (Hawaiian hot spot latitude is 19°N) the net southward motion has been very slow to negligible. It is reasonable, then, to expect that these changes in hot spot motion relative to the geomagnetic field should show up as changes in orientation and age progression along the Hawaiian-Emperor chain (vector sum of hot spot motion and Pacific plate motion).

[25] From deep drilling penetration and compositional data it is likely that the waning stage of shield formation or the postshield stage of volcano construction has now been sampled at five of the Emperor volcanoes (Detroit central, Sites 1203 and 1204; Suiko, Site 433; Nintoku, Site 1205; Ojin, Site 430; and Koko, Site 1206). Thus a revised evaluation of the age progression along the Emperor Seamounts can be done by comparing volcano ages at a common stage of construction. From a composite of dredged and drilled samples of shield, postshield and posterosional lava compositions, *Dalrymple et al.* [1980a] concluded that a linear age progression best fit the Hawaiian-Emperor chain, either 8 cm/yr for the entire lineament (Suiko to Kilauea) or a two-phase motion of 6 cm/yr (Suiko to Midway) followed by 9 cm/yr (Midway to Kilauea). *Clague and Dalrymple* [1987] amended the rates to 8.6 cm/yr for the whole chain, or their preferred two-phase motion of 6.8 cm/yr (Suiko to Laysan) and 10.1 cm/yr (Laysan to Kilauea). Neither model is especially supportive of rapid southward hot spot motion during Emperor Seamount formation or a significant change in velocity at the bend.

[26] New radiometric data from *Keller et al.* [1995] for Detroit north (81 Ma), *Sharp and Clague* [2002] for Suiko Seamount (61.3 Ma) and volcanoes in the vicinity of the Hawaiian-Emperor bend

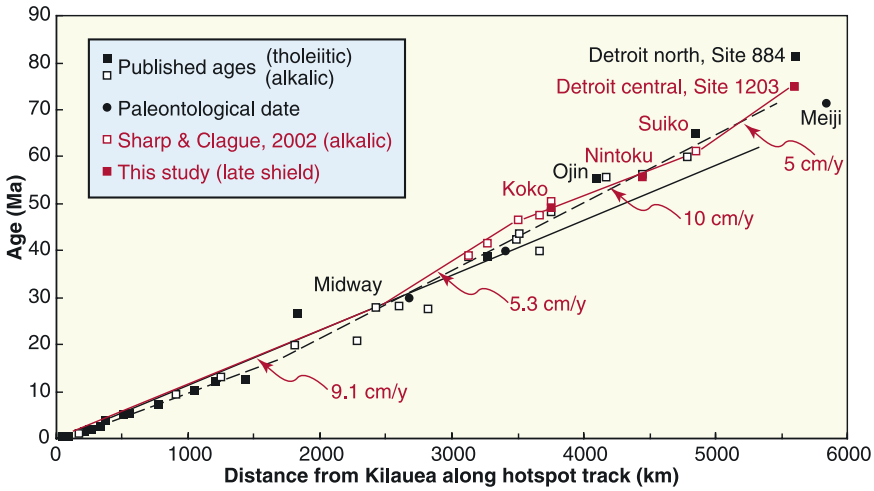

Figure 3. Age-distance relationship among volcanoes of the Hawaiian-Emperor volcanic chain. To first approximation, the trend is linear (solid black line [*Dalrymple et al.*, 1980a]) or two linear segments (dashed black line [*Clague and Dalrymple*, 1987]), but significant departures occur in the region between Detroit and Koko Seamounts, estimated visually from new radiometric dating (red symbols and solid line segments [*Sharp and Clague*, 2002; this paper]). A feature of both Emperor Seamounts and Hawaiian ridge portions of this lineament is slower followed by faster Pacific plate velocities, which may be related to plate direction changes just prior to Detroit Seamount formation and at the Hawaiian-Emperor bend. The Meiji age is a minimum age and not used in estimating age progressions. Previously reported volcano ages from *Clague and Dalrymple* [1987].

(47 Ma), and this paper, plus the evidence that the Hawaiian hot spot has moved southward at variable rates, provide new impetus for examination of the age progression along the Emperor trend and implications for Pacific plate-hot spot dynamics. For this discussion we have estimated age progression rates and provided reference lines (Figure 3) from the new data without formal statistical fitting. At this point it is clear that a constant linear rate for the whole chain is not appropriate, but final assessment of variable rates will require additional sampling of waning stage shield activity in remaining gaps (e.g., Detroit to Suiko) and high quality radiometric ages.

[27] Essentially, as noted by *Sharp and Clague* [2002], the younger age for Suiko Seamount and the older age for the bend imply a much faster age progression (~10 cm/yr) for the period 61–47 Ma and construction of the central-southern Emperor Seamounts. But the northern seamounts (Detroit central to Suiko) now reveal a much slower age progression (~5 cm/yr). Since the rate for the northern segment is not much faster than the inferred southward velocity of the hot spot, we conclude that the Pacific plate moved very slowly with respect to the Hawaiian hot spot during this period (81–61 Ma). Of course, the paleolatitude data are insensitive to longitudinal hot spot drift, and other possible hot spot motions (e.g., south-

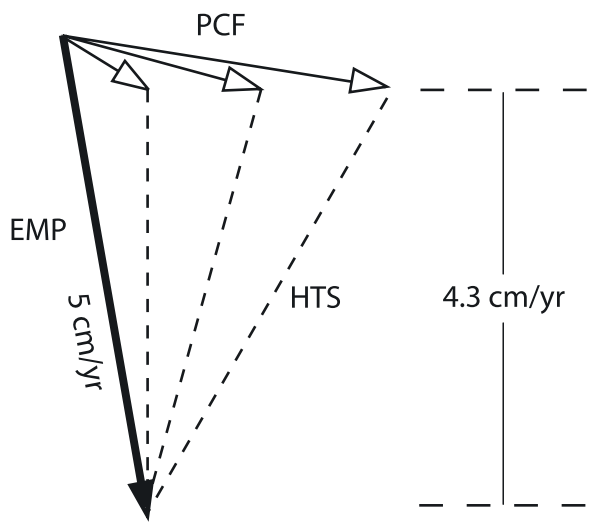

Figure 4. Vector sums of Pacific plate (PCF, light solid lines) and hot spot (HTS, dashed lines) motions, which together add to produce the observed direction and age progression within the northern Emperor Seamounts (EMP, heavy line), 81–61 Ma. Since paleolatitude data (4.3 cm/yr southward motion) are insensitive to longitudinal hot spot motion, a range of possible solutions exists, which indicate either very slow Pacific plate motion (for southward hot spot motion) or faster plate motion (for progressively greater westward hot spot motion). However, numerical convection models require south to southeasterly hot spot motion (toward the spreading ridge).

westerly) would imply faster west-northwesterly Pacific plate velocities (Figure 4). However, such hot spot drift directions would not be consistent with numerical convection models that predict lower mantle flow toward the spreading ridges [*Steinberger and O'Connell*, 1998].

[28] For the Hawaiian ridge trend the older age for the bend now implies a slower velocity (~5.3 cm/yr) for the bend-Midway segment (47–27 Ma) and 9.1 cm/yr for Midway to Kilauea. Interestingly, the two periods of slower Pacific plate motion occur after major changes in plate direction: the Meiji-Detroit segment (NW–SE) to Detroit-Suiko segment (N–S), and the southern Emperor segment (N–S) to western Hawaiian ridge segment (NNW–SSE). With the older age for the bend (*Sharp and Clague* [2002] argue that the change in plate motion direction begins with Koko Seamount) the second transition now correlates with a reorganization of seafloor spreading (chrons 22–24); such a correlation for the first transition cannot be established because it occurred within the Cretaceous long normal polarity interval. Slow-downs after plate direction changes, followed by faster velocities make kinematic sense in terms of reorganizations of subduction zones and establishment of new downgoing slabs.

[29] We can compare this revised Pacific plate-hot spot motion against the single other well-documented Pacific hot spot lineament, the Louisville Ridge, that was constructed over the same period (80–0 Ma). *Koppers et al.* [2004] have reanalyzed samples previously dated using total fusion ^{40}Ar-^{39}Ar experiments by *Watts et al.* [1988]. The new age determinations are of comparable quality and distribution to the new ages from the Emperor Seamounts (Figure 3). Curiously, the Louisville data show many of the same features as the Emperor data; namely, rather slow plate motion (2.9 cm/yr) during 80–61 Ma, followed by faster motion (6.7 cm/yr) during 61–47 Ma. A second slower period (47–25 Ma) is possible but not required by the few data available. There are no paleolatitude data from the Louisville chain to assess hot spot motion independently. These common features of geometry and timing could support the idea of Pacific plate motion over two long-lived hot spots that are fixed with respect to one another. However, the most recent attempts to fit these lineaments with a set of stage poles for Pacific-hot spot motion, with Hawaii and Louisville hot spots fixed, have failed for the older parts (80–47 Ma) of the chains [*Steinberger et al.*, 2004]. Allowing the hot spots to move in a mantle flow constrained by global plate motions produces a model that successfully matches the observed age progressions [*Koppers et al.*, 2004]. In this model, for the period 80–47 Ma, the Hawaiian hot spot moved south rapidly, consistent with the paleolatitude results of *Tarduno et al.* [2003], while the Louisville hot spot moved only slowly, so the distance between the two hot spots decreased. After 47 Ma the hot spots maintained a nearly fixed geometry.

Acknowledgments

[30] We thank the officers and crew of the R/V JOIDES Resolution for their professional expertise and sharing their home with us at sea. John Huard assisted with sample preparation and laser heating analyses, and keeping the mass spectrometer in excellent working order. We benefited from the comments of reviewers Paul Layer, Warren Sharp, and Associate Editor John Tarduno. Both authors were supported by the JOI/USSSP in this postcruise science and in participation in Leg 197 of the Ocean Drilling Program.

References

Berggren, W. A., D. V. Kent, C. C. Swisher, and M.-P. Aubry (1995), A revised Cenozoic geochronology and chronostratigraphy, in *Geochronology, Time Scales and Global Stratigraphic Correlation*, edited by W. A. Berggren, D. V. Kent, and J. Hardenbol, *Spec. Publ. SEPM Soc. Sediment. Geol.*, *54*, 129–212.

Clague, D. A., and G. B. Dalrymple (1973), Age of Koko Seamount, Emperor seamount chain, *Earth Planet. Sci. Lett.*, *17*, 411–415.

Clague, D. A., and G. B. Dalrymple (1987), The Hawaiian-Emperor volcanic chain, Part I, Geologic evolution, *U.S. Geol. Surv. Prof. Pap.*, *1350*, 5–54.

Creager, J. S., et al. (1973), *Initial Reports of the Deep Sea Drilling Program*, vol. 19, U.S. Govt. Print. Off., Washington, D. C.

Dalrymple, G. B., M. A. Lanphere, and D. A. Clague (1980a), Conventional and ^{40}Ar/^{39}Ar K-Ar ages of volcanic rocks from Ojin (Site 430), Nintoku (Site 432) and Suiko (Site 433) seamounts and the chronology of volcanic propagation along the Hawaiian-Emperor Chain, *Initial Rep. Deep Sea Drill Proj.*, *55*, 659–676.

Dalrymple, G. B., M. A. Lanphere, and J. H. Natland (1980b), K-Ar minimum age for Meiji Guyot, Emperor seamount chain, *Initial Rep. Deep Sea Drill. Proj.*, *55*, 677–683.

Duncan, R. A. (2001), A time frame for construction of the Kerguelen Plateau and Broken Ridge, *J. Petrol.*, *43*, 1109–1119.

Keller, R. A., M. R. Fisk, and R. A. Duncan (1995), Geochemistry and ^{40}Ar/^{39}Ar geochronology of basalts from ODP Leg 145, *Proc. Ocean Drill. Program Sci. Results*, *145*, 333–344.

Koppers, A. A. P. (2002), ArArCALC—Software for Ar-40/Ar-39 age calculations, *Comput. Geosci.*, *28*, 605–619.

Koppers, A. A. P., R. A. Duncan, and B. Steinberger (2004), Implications of a nonlinear $^{40}Ar/^{39}Ar$ age progression along the Louisville seamount trail for models of fixed and moving hot spots, *Geochem. Geophys. Geosyst.*, *5*, Q06L02, doi:10.1029/2003GC000671.

Min, K. W., R. Mundil, P. R. Renne, and K. R. Ludwig (2000), A test for systematic errors in $^{40}Ar/^{39}Ar$ geochronology through comparison with U/Pb analysis of a 1.1-Ga rhyolite, *Geochim. Cosmochim. Acta*, *64*, 73–98.

Pringle, M. S., and R. A. Duncan (1995), Radiometric ages of basaltic lavas recovered at Sites 865, 866 and 869, *Proc. Ocean Drill. Program Sci. Results*, *143*, 277–283.

Renne, P. R., C. C. Swisher, A. L. Deino, D. B. Karner, T. L. Owens, and D. J. DePaolo (1998), Intercalibration of standards, absolute ages and uncertainties in $^{40}Ar/^{39}Ar$ dating, *Chem. Geol.*, *145*, 117–152.

Sharp, W. D., and D. A. Clague (2002), An older, slower Hawaii-Emperor Bend, *Eos Trans. AGU*, *83*(47), Fall Meet. Suppl., Abstract T61C-04.

Shipboard Scientific Party (2002), Leg 197 summary, *Proc. Ocean Drill. Program Initial Results*, *197*, 1–92.

Steiger, R. H., and E. Jager (1977), Subcommission on geochronology: Convention on the use of decay constants in geo- and cosmochronology, *Earth Planet. Sci. Lett.*, *36*, 359–362.

Steinberger, B., and R. J. O'Connell (1998), Advection of plumes in mantle flow: Implications for hotspot motion, mantle viscosity and plume distribution, *Geophys. J. Int.*, *132*, 412–434.

Steinberger, B., R. Sutherland, and R. J. O'Connell (2004), Prediction of Emperor-Hawaii seamount locations from a revised model of global plate motion and mantle flow, *Nature*, *430*, 167–173.

Tarduno, J., et al. (2003), The Emperor Seamounts: Southward motion of the Hawaiian hotspot plume in Earth's mantle, *Science*, *301*, 1064–1069.

Watts, A. B., J. K. Weissel, R. A. Duncan, and R. L. Larson (1988), Origin of the Louisville Ridge and its relationship to the Eltanin fracture zone system, *J. Geophys. Res.*, *93*, 3051–3077.

York, D. (1969), Least squares fitting of a straight line with correlated errors, *Earth Planet. Sci. Lett.*, *5*, 320–324.